Full Paper

Propellants, Explosives, Pyrotechnics

DOI: 10.1002/prep.201800260

Shock Initiation of Nano-TATB Explosives under Short-Duration Pulses

Xiangli Guo,[a] Jun Wang,*[a] Jianlong Ran,[a] Lulu Zhao,[a] Yong Han,[a] and Wei Cao*[a]

Abstract: Because of the potential of nano-TATB as a charge in slapper detonator, the shock initiation threshold of nano-TATB explosive was studied over short pulse durations (down to 0.017 μs) and high pressure ranges (up to 17 GPa). The pulses were produced by the impact of thin plastic flyer plates, which were accelerated by electrically exploded metal foils. Nano-TATB powders with a mean particle size of 60 nm were prepared and pressed into cylindrical sample charges with three densities (1.56, 1.64 and 1.74 g/cm^3). The flyer impact velocity data versus charging voltages was measured with different flyer thicknesses. Together with the Hugoniot relationships of flyer and samples, the impact pressures and pulse durations were calculated. By using Langlie method, the threshold pressures for shock initiation were determined. In case of the identical flyer plate, the threshold pressure increases with increasing density. In case of the identical explosive density, the threshold pressure increases as the thickness of the flyer decreases (i.e. the pulse duration decreases) except for the highest tested density. These data are represented well by a constant $P^2\tau$ initiation criterion for the short, high-pressure pulses and deviate from the $P^2\tau$ behavior at lower pressures. Finally, nano-TATB is proved to be a little more sensitive to short-duration pulses than superfine TATB, but much more sensitive than production grade TATB.

Keywords: shock initiation · nano-TATB · flyer impact · short-duration pulse · threshold pressure

1 Introduction

2,4,6-Triamino-1,3,5-trinitrobenzene (TATB) is a well-known insensitive explosive as it satisfies the safety requirements at high temperature and its resistance to accidental initiation and explosion. Thus, TATB is widely used in modern nuclear warheads and robust munitions in the military, also in deep oil well explorations in the civilian application [1]. Moreover, ultrafine TATB (an arithmetic mean particle size of about 10 μm) has been proved to be more sensitive to a short, high-pressure pulse [2], thus it has more potential in slapper detonators if TATB powders are made to meet certain purity and surface area specifications.

In the field of energetic materials, nano-structured components are of great importance for applications because the sensitivity and performance are strongly changed when the particle size is reduced to nanometer-scale [3–6]. Nano-HNS (2,2′,4,4′,6,6′-hexanitrostilbene) has been proved to be more sensitive than HNS-IV (ultrafine HNS) under a short-duration pulse [7]. While nano-TATB has been prepared in many literatures in the past more than ten years [8–12], its sensitivity to a short-duration and high-pressure impact is unclear. Therefore, its potential as a charge in slapper detonators is unrevealed.

For the high-velocity impact, the short duration (less than a few microseconds) and high pressure (2 GPa and higher) of initial shock waves are sufficient to induce detonation rapidly [13]. In order to study the response of nano-TATB under high-pressure and short-duration impulses, a high-velocity flyer plate impacting on the target is essential. The electric gun, which is widely used in shock initiation of explosives [14–20], was utilized to accelerate the flyer in this work. The electric gun is developed by the Lawrence Livermore National Laboratory [14], which operates by electrically exploding a metal foil that accelerates a plastic flyer plate to high velocity. When the flyer impacts with a target, a well-characterized shock is produced. Thus, it is a good method of studies on shock initiation, which requires a pressure pulse of known amplitude and duration. In addition, compared with the traditional means of accelerating flyer plates with a gas gun or explosive planar wave lens, electric gun is time-saving and low-cost.

In this paper, the nano-TATB was prepared and pressed into cylindrical tablets with three different densities. The charges were impacted with high-velocity flyer plates accelerated by an electric gun. The initiation threshold pressures were determined and the shock initiation characteristics of the charges were analyzed for different densities, different flyer thicknesses and different particle sizes, respectively. Then the sensitivities of nano-TATB to short-duration pulses was compared to those of other grain-size TATBs.

[a] *X. Guo, J. Wang, J. Ran, L. Zhao, Y. Han, W. Cao*
Institute of Chemical Materials
China Academy of Engineering Physics
P.O. Box 919-319, Mianyang, Sichuan 621999, China
**e-mail: wjun927@caep.cn*
weicao@caep.cn

2 Experimental Section

2.1 Explosive Samples Preparation

Nano-TATB powders were prepared by solvent/nonsolvent recrystallization with concentrated sulfuric acid as solvent and deionized water as nonsolvent [8].The morphology was characterized by Zeiss Ultra 55 field emission scanning electron microscopy (SEM) and shown in Figure 1. The arithmetic mean particle size was calculated to be 60 ($\pm$0.5) nm by means of counting more than 300 particles from the obtained SEM image via the statics of the Smile View software, and Brunauer-Emmett-Teller (BET) specific surface area was determined to be 25 m^2/g. Then the nanometer powders were pressed to cylindrical charges with a dimension of Φ10 mm $\times$ 5 mm and densities of 1.56, 1.64 and 1.74 ($\pm$ 0.005) g/cm^3. Theoretical maximum density (TMD) of TATB is 1.937 g/cm^3 [21], thus the charge porosities $n = 1-\rho/\rho_{TMD}$ are 0.195, 0.153 and 0.102, respectively. All the explosives were produced and prepared by Institute of Chemical Materials, China Academy of Engineering Physics (CAEP).

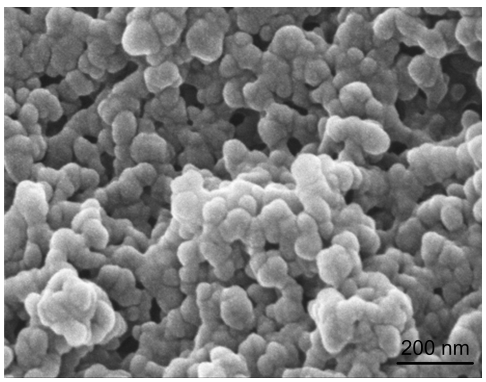

Figure 1. SEM image of nano-TATB powders.

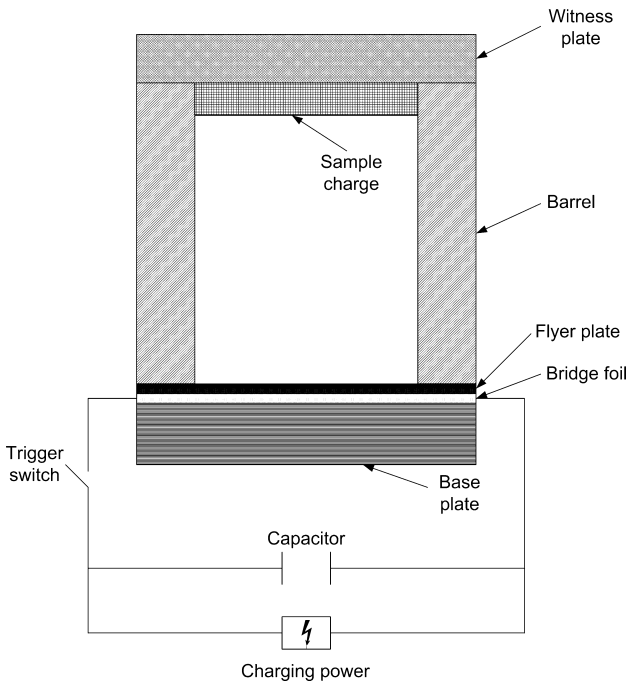

Figure 2. Sketch of the experimental setup.

2.2 Shock Initiation Threshold Measurements

The use of the electric gun for determination of shock-initiation threshold has been described in details elsewhere [15], so just a brief description of its operation is given here. The electric gun uses a capacitor bank discharge to explode an aluminum foil. The foil plasma drives a thin Mylar polyester flyer up a PMMA (polymethylmethacrylate) barrel to impact a high explosive target. The flyer layer is sheared by the edge of the inner diameter of the barrel which is clamped onto the flyer laminate, thus the diameter of the flyer is defined by the inner diameter of the barrel. The crater is viewed on a witness plate (Q235 steel, 16 mm $\times$ 16 mm $\times$ 5 mm) to determine whether a full detonation has occurred or not. The experimental setup is schematically shown in Figure 2. The choice of foil and flyer dimensions depends on the area one wishes to impact and the desired magnitude and duration of the pressure pulse. The flyer velocity is determined by the selection of barrel length, bank charging voltage (burst current density), foil thickness and flyer thickness. In this work, three flyer thickness values (0.05, 0.1 and 0.2 mm) were chose to get three different durations of the pressure pulse introduced into the samples. For the thickest flyer (0.2 mm), the aluminum foil was also thickened to 0.025 mm, from 0.01 mm which was used for the other flyers. The electric gun is made by Institute of Fluid Physics, CAEP [22], and the parameters of it are listed in Table 1.

In order to determine a fully established detonation response, the following two conditions should be fulfilled simultaneously. First, a significant punching imprint is on the witness plate and the diameter of the imprint should be larger than that of the charge, or a hole is punched through the witness plate (i.e. the witness plate is holed). Secondly, no explosive residual is left over the witness plate. For rou-

Table 1. Parameters of the electric gun.

Parameter	Value
Capacitance	32 μF
Resistance	20 mΩ
Inductance	32 nH
Maximum voltage	40 kV
Mylar flyer plate (thickness)	0.05, 0.1, 0.2 mm
Aluminum foil	16 mm $\times$ 16 mm $\times$ 0.01
(length $\times$ width $\times$ thickness)	(or 0.025) mm
Barrel	Φ10 mm $\times$ 5 mm
Planarity	$\leq$ 34 ns

tine initiation experiments, we usually measured a threshold voltage for initiation, which could be converted to a threshold velocity through our calibrations. Bank charging voltages are more easily and accurately measured. The voltage threshold for shock initiation at 50% probability was determined by Langlie method [23]. A calibration curve of flyer plate velocity versus bank charging voltage was measured by a Doppler laser-interference velocimeter with measuring accuracy of 1~2% [24] provided by Institute of Fluid Physics, CAEP.

3 Results and Discussion

3.1 Flyer Plate Velocity and Impact Pressure Calibration

Using the Doppler laser-interference velocimeter, we obtained the velocity histories of the flyer plates for various charging voltages and flyer thicknesses. Figure 3 shows the typical velocity and displacement histories (closing the switch of electric gun is defined as time zero). Considering the length of barrel is 5 mm, we can easily find the impact velocity corresponding to this displacement (shown as dotted lines in Figure 3).

A part of the flyer impact velocity data versus charging voltages measured for various flyer thicknesses is shown in Figure 4, which includes the threshold values used below in this work. The trend is clearly shown that the impact velocity increases as the increase of charging voltage, and the flyer with smaller thickness has a higher impact velocity.

The results of these experiments were analyzed by using standard analytic procedures to calculate the pressure created by flyer impact with the explosive samples. For these analyses it was assumed that the shock velocity could be expressed in the form of experimental Hugoniot data represented by linear shock relation as follows:

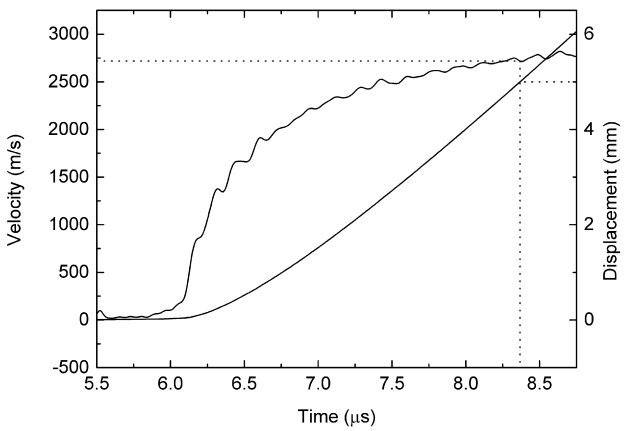

Figure 3. Velocity and displacement histories of the flyer plate (charging voltage 9.21 kV, flyer thickness 0.2 mm).

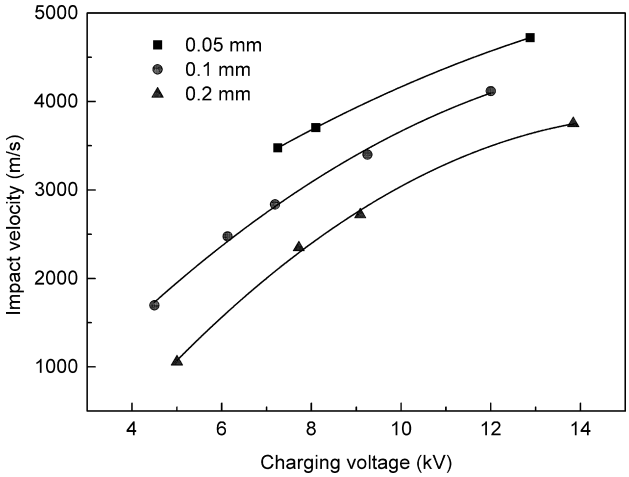

Figure 4. Impact velocity versus charging voltage for various flyer thicknesses.

$$U_s = C_0 + SU_p, \quad (1)$$

where U_s is the shock velocity, C_0 is the hydrodynamic sound speed, S is a material constant, and U_p is the particle velocity. To compute stresses and pulse lengths, we used published data for the Hugoniot curves of Mylar [14], and experimental Hugoniot data of the TATB samples. The experimental Hugoniot data was measured by shock wave experiments at pressure range between 2 and 14 GPa. Experiments were conducted in Southwest Jiaotong University, China and the experimental procedure was described in [25] with a different target. The values used for these parameters are shown in Table 2, with the initial density ρ_0 for each material.

When a flyer collides with a target material, both impinging pressures of the flyer and target are equal due to pressure continuity. The relationship between impact velocity and pressure is derived by combining the momentum conservation equation and linear shock relation as follows:

$$P_i = \rho_{0,T}(C_{0,T} + S_T U_{p,T})U_{p,T} = \rho_{0,F}(C_{0,F} + S_F U_{p,F})U_{p,F}, \quad (2)$$

$$U_{p,T} = V_F - U_{p,F}, \quad (3)$$

where P_i and V_F are the impact pressure and flyer impact velocity respectively. Subscripts T and F represent the prop-

Table 2. Parameters of the Hugoniot curves.

Material	ρ_0 (g/cm3)	C_0 (km/s)	S
Mylar	1.40	2.54	1.49
TATB	1.56	0.655	2.971
TATB	1.64	0.765	2.724
TATB	1.74	1.465	2.434

Table 3. Threshold pressures and pulse durations for various conditions.

ρ_0 (g/cm^3)	$d_F = 0.05$ mm		$d_F = 0.1$ mm		$d_F = 0.2$ mm	
	P (GPa)	τ (μs)	P (GPa)	τ (μs)	P (GPa)	τ (μs)
1.56	13.793	0.0188	7.920	0.0451	7.280	0.0924
1.64	15.318	0.0182	9.873	0.0421	9.229	0.0860
1.74	16.837	0.0176	13.248	0.0382	15.544	0.0723

erties of the target and flyer respectively. Combining Eqs. (2) and (3), we get the values of P_i and $U_{p,F}$.

The impact of an aluminum flyer upon a charge generates a rectangular pressure pulse [26]. An exact value for the duration of the shock is not obtainable but an approximate value is the time required for a shock to travel twice the thickness of the flyer:

$$\tau = 2d_F/U_{s,F}, \quad (4)$$

where τ is the pulse duration, and d_F is the thickness of the flyer.

Using the method introduced above, we measured the threshold impact velocity corresponding to the threshold charging voltage. Then the threshold pressure P and pulse duration τ were calculated and listed in Table 3.

3.2 Shock Sensitivity Analysis

Shock sensitivity problem of high explosives (HE) is essentially shock-to-detonation-transition (SDT) problem. Modern scheme of SDT process consists of two stages [27]. During the first stage, the energy supplied by the shock causes irreversible deformation of the porous explosive material and formation of "hot spots" or local dynamically overheated regions. Hot spots growth and coalescence result in detonation buildup during the second stage of SDT process.

Figure 5 shows the threshold pressure versus density data for various flyer thicknesses. In case of the identical flyer plate, the value of threshold pressure increases with the density. This can be simply explained on the basis of the first stage of SDT. Namely, the sensitivity of HE to shock ignition grows when HE porosity increases. In this ignition phase, the SDT process depends primarily on total void volume and is controlled by hot spot formation rate. The larger the total void volume, the lower the shock pressure required for ignition.

In case of the identical explosive density, the threshold pressure increases as the thickness of the flyer decreases except for $\rho_0 = 1.74$ g/cm^3. Since $U_{s,F}$ changes very slowly with varied P_i among the measuring range, the increasing flyer thickness d_F is approximately equivalent to the rising shock pulse duration τ. Thus this implies that the nano-TATB explosive charge is less sensitive with shorter shock pulse duration. Even for the case of $\rho_0 = 1.74$ g/cm^3, the specimen is

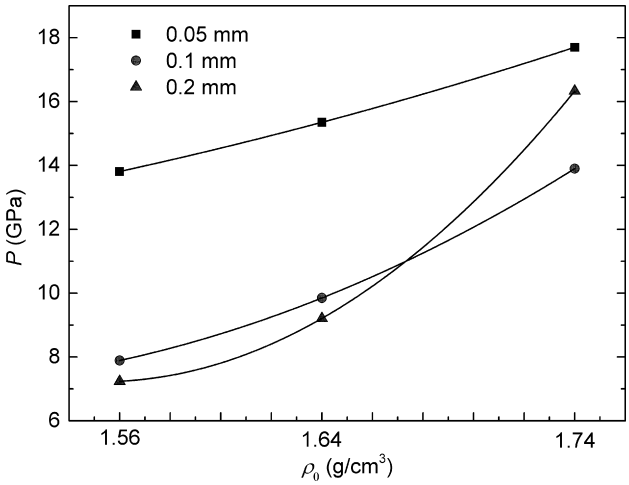

Figure 5. Threshold pressure-density data for various flyer thicknesses.

the least sensitive with 0.05 mm-thick flyer (i.e. the shortest shock pulse duration); nevertheless, we did not know why the specimen is less sensitive with 0.1 mm-thick flyer than that with 0.2 mm-thick flyer. With even higher density, we plan to study in the future.

In Figure 6 we illustrate the initiation thresholds in terms of pressure and pulse length for the samples on a log-log axis system in this study, together with other TATB formulations' shock initiation data obtained by electric gun in [16]. These formulations include production grade (B-226, BET specific surface area 0.539 m^2/g, arithmetic mean particle size 58 μm), superfine (B-474, 0.513 m^2/g, 17 μm), and ultrafine (B-592, 4.323 m^2/g, 9 μm) crystal size TATBs. In spite of different densities, comparison of the nano-TATB ini-

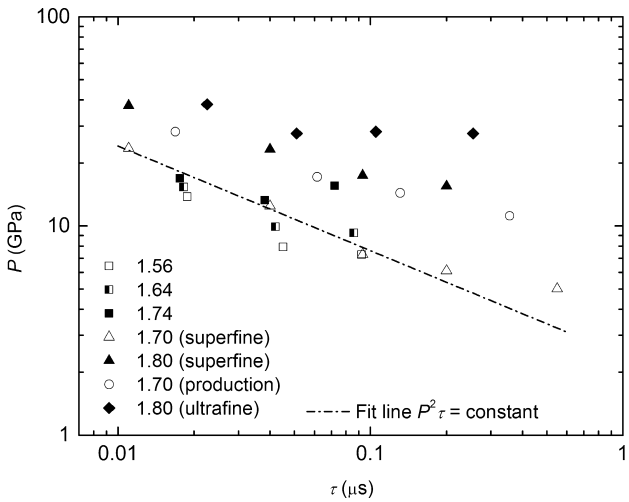

Figure 6. Threshold pressure-pulse duration data for various formulations and tested densities (the numbers showed in the legend are densities in g/cm^3).

tiation data with those for larger particle-size samples, the same trend is that the threshold pressure increases as the pulse duration decreases for most formulations, especially among the shorter, higher-pressure pulse range.

We also drew a straight line in the form of $P^2\tau =$ constant as the fit line for the formulations in Figure 6 to help us understand the trend of the data. Despite of limited data points in our study, the nano-TATB was observed to follow a minimum $P^2\tau$ initiation criterion for the short, high-pressure pulses and deviate from the $P^2\tau$ behavior at lower pressures. This phenomenon is the same as other TATB formulations in Figure 6. A constant $P^2\tau$ initiation threshold has also been observed for PBX-9404 (94% HMX, 3% NC, 3% tris(2-chloroethyl)phosphate) and Comp. B-3 (60% RDX, 40% TNT) [24] and a number of papers discussed different mechanisms to explain and extend this relationship [28–31].

Simply applying the interpolation approach to the constant $P^2\tau$ value, the $P^2\tau = 5.802\ \mathrm{GPa^2\,\mu s}$ was calculated for nano-TATB at 1.70 g/cm^3. Comparing to $P^2\tau = 6.136\ \mathrm{GPa^2\,\mu s}$ for superfine TATB and $16.080\ \mathrm{GPa^2\,\mu s}$ for production grade TATB in Figure 6, the nano-TATB is a little more sensitive than superfine TATB but much more sensitive than production grade TATB under short-duration pulses.

4 Conclusions

The shock initiation thresholds of nano-TATB explosives have been studied over the pressure range of 7–17 GPa with pulse duration ranging from 0.017–0.093 μs. The high-pressure and short-duration pulses were generated by the impact of thin plastic flyer plates that accelerated by electrically exploded metal foils. The charges were pressed into cylinders with dimension of $\Phi 10\ \mathrm{mm} \times 5\ \mathrm{mm}$ and three densities from nano-TATB powders with a mean particle size of 60 nm. We performed the experiments with flyer thicknesses of 0.05 mm, 0.1 mm and 0.2 mm.

The flyer impact velocity data versus charging voltage was measured for various flyer thicknesses, higher charging voltage and thinner flyer plate result in a higher impact velocity. Together with the Hugoniot relationships of flyer and samples, the impact pressures and pulse durations were calculated. By using Langlie method, the threshold pressures for shock initiation were determined. Results show that in case of the identical flyer plate, the value of threshold pressure increases with increasing density. In case of the identical explosive density, the threshold pressure increases as the thickness of the flyer decreases (i.e. the pulse duration decreases) except for $\rho_0 = 1.74$ g/cm^3. The nano-TATB was observed to follow a minimum $P^2\tau$ initiation criterion for the short, high-pressure pulses and deviate from the $P^2\tau$ behavior at lower pressures. Compared with other TATB at the same density of 1.70 g/cm^3, nano-TATB is a little more sensitive than superfine TATB, but much more sensitive than production grade TATB under short-duration pulses.

Further research needs to be conducted to get more short and high-pressrue shock initiation data of nano-TATB charges for higher explosive density and wider pressure range, and optimize all other parameters relating with the shock initaiton to realize the potential of nano-TATB in slapper detonators.

Acknowledgements

We gratefully acknowledge the support and encouragement of Dr. Shanggang Wen. This research is funded by National Natural Science Foundation of China (Nos. 11702265, 11602238).

References

[1] V. M. Boddu, D. S. Viswanath, T. K. Ghosh, R. Damavarapu, 2,4,6-Triamino-1,3,5-trinitrobenzene (TATB) and TATB-based formulations – A review, *J. Hazard. Mater.* **2010**, *181*, 1–8.
[2] R. Lee, G. Bloom, W. Von Holle, W. Weingart, L. Erickson, S. Sanders, C. Slettevold, R. McGuire, Relationship between the shock sensitivity and the solid pore sizes of TATB powders pressed to various densities, *8th Symposium (International) on Detonation*, Albuquerque, New Mexico, USA, 15–19 July, **1985**, p. 3–14.
[3] Y. Bayat, V. Zeynali, Preparation and characterization of nano-CL-20 explosive, *J. Energ. Mater.* **2011**, *29*, 281–291.
[4] J. Liu, W. Jiang, F. Li, L. Wang, J. Zeng, Q. Li, Y. Wang, Q. Yang, Effect of drying conditions on the particle size, dispersion state, and mechanical sensitivities of nano HMX, *Propellants Explos. Pyrotech.* **2014**, *39*, 30–39.
[5] Q. Peng, W. Cao, W. Zhou, Z. He, W. Jiang, W. Chen, Electrostatic Hazards Assessment of Nitramine Explosives: Resistivity, Charge Accumulation and Discharge Sensitivity, *Cent. Eur. J. Energ. Mater.* **2016**, *13*, 755–769.
[6] N. Zohari, M. H. Keshavarz, S. A. Seyedsadjadi, The advantages and shortcomings of using nano-sized energetic materials, *Cent. Eur. J. Energ. Mater.* **2013**, *10*, 135–147.
[7] C. An, S. Xu, Y. Zhang, B. Ye, X. Geng, J. Wang, Nano-HNS Particles: Mechanochemical Preparation and Properties Investigation, *J. Nanomater.* **2018**, *2018*, 9436089.
[8] G. Yang, F. Nie, H. Huang, L. Zhao, W. Pang, Preparation and Characterization of Nano-TATB Explosive, *Propellants Explos. Pyrotech.* **2006**, *31*, 390–394.
[9] L. Yang, X. Ren, T. Li, S. Wang, T. Zhang, Preparation of ultrafine TATB and the technology for crystal morphology control, *Chin. J. Chem.* **2012**, *30*, 293–298.
[10] X. Tan, X. Duan, C. Pei, H. Xu, Preparation of nano-TATB by semi-batch reaction crystallization, *Nano* **2013**, *8*, 1350055.
[11] Y. Lei, J. Wang, C. An, Nano 1,3,5-triamino-2,4,6-trinitro-benzene particles prepared by "green" recrystallization, *Sci. Technol. Energ. Mater.* **2014**, *75*, 174–178.
[12] Y. Wang, J. Wang, G. Yang, Preparation of nano-TATB from CF_3SO_3H/H_2O by spraying crystallization, *Chin. J. Energ. Mater.* **2016**, *24*, 969–972.
[13] A. W. Campbell, W. C. Davis, J. B. Ramsay, J. R. Travis, Shock initiation of solid explosives, *Phys. Fluids* **1961**, *4*, 511–521.
[14] R. Weingart, R. Lee, R. Jackson, N. Parker, Acceleration of thin flyers by exploding metal foils: application to initiation studies, *6th Symposium (International) on Detonation*, Coronado, California, USA, 24–27 August, **1976**, p. 653–663.

[15] R. Weingart, R. Jackson, C. Honodel, R. Lee, Shock Initiation of PBX-9404 by electrically driven flyer plates, *Propellants Explos. Pyrotech.* **1980**, *5*, 158–162.
[16] C. Honodel, J. Humphrey, R. Weingart, R. Lee, P. Kramer, Shock initiation of TATB formulations, *7th Symposium (International) on Detonation*, Annapolis, Maryland, USA, 16–19 June, **1981**, p. 425–434.
[17] W. Seitz, Short-duration shock initiation of triaminotrinitrobenzene (TATB), in: *Shock Waves in Condensed Matter 1983* (Eds.: R. A. Graham, G. K. Straub), Elsevier, Amsterdam **1984**, p. 531–534.
[18] G. Wang, C. Sun, J. Chen, C. Liu, J. Zhao, F. Tan, N. Zhang, Large area and short-pulse shock initiation of a TATB/HMX mixed explosive, *AIP Conf. Proc.* **2007**, *955*, 1014–1017.
[19] A. K. Saxena, T. C. Kaushik, S. C. Gupta, Shock experiments and numerical simulations on low energy portable electrically exploding foil accelerators, *Rev. Sci. Instrum.* **2010**, *81*, 033508.
[20] H. Yu, B. Kim, S. Jang, K. Kim, J. J. Yoh, Performance characterization of a miniaturized exploding foil initiator via modified VISAR interferometer and shock wave analysis, *J. Appl. Phys.* **2017**, *121*, 215901.
[21] H. H. Cady, A. C. Larson, The crystal structure of 1, 3, 5-triamino-2, 4, 6-trinitrobenzene, *Acta Crystallogr.* **1965**, *18*, 485–496.
[22] G. Wang, J. He, J. Zhao, F. Tan, C. Sun, J. Mo, X. Xong, G. Wu, The techniques of metallic foil electrically exploding driving hypervelocity flyer to more than 10 km/s for shock wave physics experiments, *Rev. Sci. Instrum.* **2011**, *82*, 095105.
[23] MIL-STD-331D, Fuzes, Ignition Safety Devices and Other Related Components Environmental and Performance Tests for, Washington, D. C., USA, Department of Defense **2017**.
[24] J. Weng, H. Tan, X. Wang, Y. Ma, S. Hu, X. Wang, Optical-fiber interferometer for velocity measurements with picosecond resolution, *Appl. Phys. Lett.* **2006**, *89*, 3.
[25] X. Huang, X. Yuan, Z. Chen, F. Liu, W. Bai, Hugoniot equation of state of olivine and its geodynamic implications, *Sci. China: Earth Sci.* **2016**, *59*, 619–625.
[26] Y. de Longueville, C. Fauquignon, H. Moulard, Initiation of several condensed explosives by a given duration shock wave, *6th Symposium (International) on Detonation*, Coronado, California, USA, 24–27 August, **1976**, p. 105–114.
[27] B. A. Khasainov, B. S. Ermolaev, H.-N. Presles, P. Vidal, On the effect of grain size on shock sensitivity of heterogeneous high explosives, *Shock Waves* **1997**, *7*, 89–105.
[28] D. Hayes, A $P^n t$ detonation criterion from thermal explosion theory, *6th Symposium (International) on Detonation*, Coronado, California, USA, 24–27 August, **1976**, p. 76–81.
[29] J. B. Ramsay, Short-duration shock-wave initiation of solid explosives, *Acta Astronaut.* **1979**, *6*, 771–783.
[30] H. James, An extension to the critical energy criterion used to predict shock initiation thresholds, *Propellants Explos. Pyrotech.* **1996**, *21*, 8–13.
[31] P. C. Souers, P. Vitello, Initiation threshold pressures from three sources, *Propellants Explos. Pyrotech.* **2007**, *32*, 288–295.

Manuscript received: August 24, 2018
Revised manuscript received: October 6, 2018
Version of record online: January 11, 2019

